Vol. 83 No. 2 pp. 238–244 ACTA GEOLOGICA SINICA April 2009

Lisiguangite, $CuPtBiS_3$, a New Platinum-Group Mineral from the Yanshan Mountains, Hebei, China

YU Zuxiang[1,*], CHENG Fanyun[1] and MA Hongwei[2]

1 *Institute of Geology, Chinese Academy of Geological Science, Beijing 100037, China*
2 *Institute of Chemistry, the Chinese Academy of Sciences, Beijing 100082, China*

Abstract: Lisiguangite, $CuPtBiS_3$, is a new mineral species discovered in a PEG-bearing, Co-Cu sulfide vein in garnet pyroxenite of the Yanshan Mountains, Chengde Prefecture, Hebei Province, China. It is associated with chalcopyrite and bornite, galena, minor pyrite, carrolite, molybdenite and the platinum-group minerals daomanite ($CuPtAsS_2$), Co-bearing malanite ($Cu(Pt, Co)_2S_4$) sperrylite, moncheite, cooperite and malyshevite ($CuPdBiS_3$), rare damiaoite (Pt_2In_3) and yixunite (Pt_3In). Lisiguangite occurs as idiomorphic crystals, tabular or lamellae (010) and elongated [100] or as aggregates, up to 2 mm long and 0.5 mm wide. The mineral is opaque, has lead-gray color, black streak and metallic luster. The mineral is non-fluorescent. The observed morphology displays the following forms: pinacoids {100}, {010}, {001}, and prism {110}. No twining is observed. The a:b:c ratio, calculated from unit-cell parameters, is 0.6010:1:0.3836. Cleavage: {010} perfect, {001} distinct, {100} may be visible. H Mohs: $2^1/_2$; VHN_{25}=46.7-49.8 (mean 48.3) kg/mm^2. Tenacity: brittle. Lisiguangite is bright white with a yellowish tint. In reflected light it shows neither internal reflections nor bireflectance or pleochroism. It has weak to moderate anisotropy (blue-greenish to brownish) and parallel-axial extinction. The reflectance values in air (and in oil) for R_3, R_4 and ($^{im}R_3$, $^{im}R_4$), at the standard Commission on Ore Mineralogy wavelengths are: 37.5, 35.7 (23.4, 22.3) at 470 nm; 38.6, 36.5 (23.6, 22.6) at 546 nm; 39.4, 37.5 (23.6, 22.7) at 589 nm and 40.3, 38.2 (23.7, 22.9) at 650 nm. The average of eight electron-microprobe analyses: Cu 12.98, Pt 30.04, Pd 2.69, Bi 37.65 and S 17.55, totaling 100.91%, corresponding to $Cu_{1.10}(Pt_{0.83}, Pd_{0.14})_{\Sigma 0.97}Bi_{0.97}S_{2.96}$ based on six atoms *apfu*. The ideal formula is $CuPtBiS_3$. The mineral is orthorhombic. Space group: $P2_12_12_1$, a=7.7152(15)Å, b=12.838(3) Å, c=4.9248(10)Å, V=487.80(17)Å^3, Z=4. The six strongest lines in the X-ray powder-diffraction pattern [d in Å (I) (h k l) are 6.40(30)(020), 3.24(80)(031), 3.03(100)(201), 2.27(40)(051), 2.14(50)(250), 1.865(60)(232).

Key words: lisiguangite, $CuPtBiS_3$ new mineral species, Yanshan Mountains, Chengde, China

1 Introduction

Lisiguangite, IMA (International Mineralogical Association) no. 2007-3, was approved by the Commission on New Minerals, Nomenclature and Classification (CNMMNC). The holotype material, polished thin sections of lisiguangite, is deposited at the Geological Museum of China, Beijing under catalogue number M-11031.

The name is in honor of the renowned Chinese geologist, Professor Li Siguang (J.S. Lee) and celebrates the 120 anniversary of his birthday (1889.10.26–1971). He was minister of geology of China during 1952–1971, and also vice president of the Chinese Academy of Sciences and chairman of the China National Association of Sciences. As a founder of geomechanics, Professor Li believed that various tectonic traces are integrated results of stressing during movement. For this reason, he established the theory of "Tectonic System" and advocated researching the crust, crustal movement and the rule of mineral distribution. Furthermore, he pointed out that three settling zones of the new Cathaysian tectonic system in the eastern part of China are prospective regions for oil exploration. As a result, three large-scale petroleum fields: the Daqing, Dagang and Shengli Oil Fields were discovered one after another. His main works include *Chinese Geology*, *Introduction to Geomechanics*, *Seismological Geology*, *Astronomy*, *Geology and Paleontology*, etc.

* Corresponding author. E-mail: yuzuxiang001163.com.

2 Characteristics of the Country Rocks

The mineral occurs in platinum group element (*PGE*)-bearing Co-Cu sulfide veins, where garnet pyroxenite is distributed nearby Sandao Village (41°8′N, 117°40′E), about 250 km northeast of Beijing. Architectonically, it is situated on the margin of the Sino-Korea paraplatform.

The garnet pyroxenite has long been regarded as eclogite of regional metamorphic origin. But the authors of this paper found that after research, the region have garnet-bearing rocks in the region: in the mela garnet-bearing rock the garnet is andradite (contain 64.9 andradite, 18.8 grossular, 10.3 mangasnesian garnet, 6.0 pyrope, in mol.% total 100.0). The proxene is hedenbergite (contain 55.1 hedenbergite, 28.7 diopside, 9.8 jadeite and 6.4 other mangno-pyroxenee in mol.% total 100.0). Whereas in the mela-garnet-bearing rock, the garnet is grossular, containing 75.0 grossinlar, 17.0 andradite, 8.0% pyrope, in mol.% total 100.0). It is believed that the melo-rock is garnet pyroxenite that occurs in the contact metamorphic zone between relatively basic igneous rock and granite or gneiss, while the leuco-rock is garnet plagioclasite that occurs in the contact metamorphic zone between basic igneous rock and plagioclasite. Co-Cu-PGE-bearing sulfide veins always occur in th mela garnet rock.

3 Occurrence and Associated Minerals

Lisiguangite obtained from heavy concentrates as a constituent of crushed ores. The associated minerals are mainly chalcopyrite, bornite and galena, as well as carrolite, molybdenite, pyrite and tenoite. The platinum-group minerals (PGM) are lisiguanite, daomanite, Co-bearing malanite, sperrylite, moncheite, cooperite, damiaoite, yixunite, malyshevite, etc.

Besides separate single idiomorphic crystals (Plate I 1a–f), lisiguanite always shows intimate intergrowth with daomanite, Co-bearing malanite, malyshevite and was replaced by them (Plate II). Lisiguangite is an unstable mineral. It may disappear rapidly on the surface of ore bodies.

The study shows that the deposit belongs to contact metamorphic deposit with the orebodies occurring in exoskarn with very complicate compositions, and its mineralization can be divided into the following several stages: (1) Early high-temperature Si-skarnization stage. This stage is characterized by the forming of typical skarn minerals such anhydrous silicates as grossularite, andradite, hedenbergite, diopsite, vesuvianite etc. (2) Late high-temperature hyrdorthermal Si-skarnization stage. Hydrous silicates such as actinolite, tremolite, epidote, clinozoisite, apatite were formed during this stage. (3) Stage of formation of early sulfides related to hydrothermal hydrous silicates, including some laminated minerals such as phlogopite, moscovite, chlorite, and intergrowth minerals such as molybednite, pyrite, chalcopyrite.

Based on the observation that galena was formed in ore veins at the last stage, it is suggested that galena and ores were formed at a temperature higher than 400°C. This is a mesothermal deposit, which has a formation condition that is similar to that for minerals such as cooperite, moncheite, sperrylite, daomanite, and galena.

The contact metasomatic deposit of PGM is a new type of contact metamorphism in the world; moreover, five new minerals were discovered in this new type of deposit and is well worth seeing (Yu et al., 2002).

4 Appearance and Physical Properties

The mineral occurs as idiomorphic crystals, generally tabular or lamellae (010) and elongated along [100] (Plate IIa, b), up to 2 mm long and 0.5 mm wide. The observed morphology displays the forms: pinacoids H Mohs: $2^1/_2$. VHN_{25}=46.7–49.8 (mean 48.3) kg/mm^2. Tenacity: brittle. Cleavage: {010} perfect, {001} distinct, {100} visible. Fracture: stepped. Density (calc.)=7.42 g/cm^3 based on the empirical formula and powder data.

5 Optical Properties

In plane-polarized reflected light, lisiguangite is bright white with a yellowish tint. The mineral does not show internal reflection, bireflectance or pleochroism. Anisotropy is weak to moderate with blue-greenish to brownish colors and parallel-axial extinction. Reflectance data (R_1, R_2), (R_3, R_4) and ($^{im}R_3$, $^{im}R_4$) measured in air (and oil) are summarized in Table 1. Figure 1 shows the reflectance curves obtained

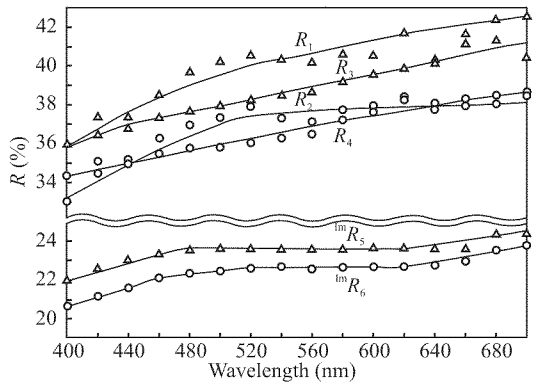

Fig. 1. R_1, R_2, R_3 and R_4 spectra (four curves in air of two grains), and $^{im}R_3$ and $^{im}R_4$ spectra of lisiguangite (two curves in oil of one grain) between 400 and 700 nm. Triangles parallel to {100} cleavage and circles perpendicular to it.

Table 1 Reflectance values (in air and oil, WTiC Standard)

Wave length	R_1/R_2	R_3/R_4	$^{im}R_3/^{im}R_4$	Wave length (nm)	R_1/R_2	R_3/R_4	$^{im}R_3/^{im}R_4$
400 nm	35.9/33.0	36.0/34.4	22.0/20.7	560	40.2/37.2	38.7/36.6	23.6/22.6
410 nm	37.2/33.8	36.3/34.8	22.3/21.0	570	40.5/37.5	39.0/37.0	23.6/22.7
420 nm	37.4/34.5	36.5/35.1	22.6/21.2	580	40.7/37.8	39.2/37.3	23.6/22.7
430 nm	37.5/34.8	36.7/35.2	23.1/21.4	**589**	**40.7/37.9**	**39.4/37.5**	**23.6/22.7**
440 nm	37.5/35.0.	36.8/35.3	23.0/21.7	600	40.6/38.0	39.6/37.7	23.8/23.0
450 nm	38.1/35.7	37.1/35.4	23.2/21.9	610	40.7/38.1	39.6/37.7	23.6/22.7
460 nm	38.6/36.3	37.3/35.5	23.3/22.1	620	40.8/38.2	39.9/38.0	23.6/22.7
470 nm	**39.2/36.7**	**37.5/35.7**	**23.4/22.3**	630	40.6/38.0	40.1/38.1	23.6/22.8
480 nm	39.8/37.0	37.7/35.8	23.5/22.4	640	40.3/37.8	40.2/38.1	23.6/22.9
490 nm	40.1/37.2	37.9/35.9	23.6/22.5	**650**	**40.8/37.9**	**40.3/38.2**	**23.7/22.9**
500 nm	40.3/37.4	38.0/35.9	23.6/22.5	660	41.2/38.0	40.3/38.2	23.8/23.0
510 nm	40.5/37.7	38.1/36.0	23.6/22.6	670	41.9/38.1	40.4/38.4	24.1/23.3
520 nm	40.6/38.0	38.2/36.1	23.6/22.7	680	42.5/38.1	40.4/38.5	24.4/23.6
530 nm	40.5/37.7	38.3/36.1	23.6/22.6	690	42.6/38.4	40.5/38.6	24.4/23.7
540 nm	40.4/37.4	38.5/36.3	23.6/22.6	700	42.7/38.6	40.5/38.7	24.4/23.8
546 nm	**40.3/37.3**	**38.6/36.5**	**23.6/22.6**				

Values shown in bold are those recommended by COM (the IMA Commission on Ore Mineralogy)

Table 2 Color values for lisiguangite

Color values relative to the CIE illuminant E						
x	0.3353	0.3377	0.3393	0.3395	0.3362	0.3348
y	0.3415	0.3397	0.3371	0.3381	0.3377	0.3362
y%	40.47	37.63	36.83	38.87	22.64	23.60
λd	563.46	573.47	584.1	581.25	573.1	570.35
Pe%	0.015	0.031	0.031	0.033	0.022	0.005
Color values for lisiguangite relative to the CIE illuminant A						
x	0.4544	0.4508	0.4532	0.4531	0.4497	0.4486
y	0.4086	0.4096	0.4076	0.4983	0.4089	0.4085
y%	40.51	37.69	37.01	39.05	22.66	23.61
λd	589.44	583.4	591.5	589.73	583.72	581.1
Pe%	0.008	0.005	0.01	0.043	0.024	0.014
Color values for lisiguangite relative to the CIE illuminant C						
x	0.3143	0.3143	0.3158	0.3159	0.3128	0.3115
y	0.3231	0.3225	0.3198	0.3210	0.3203	0.3188
y%	40.43	37.59	36.76	38.81	22.62	23.59
λd	512.15	572.35	584.42	567.36	572.31	569.95
Pe%	0.0091	0.0086	0.025	0.043	0.018	0.011

Table 3 Average and ranges of eight microprobe analyses of lisiguangite

Element	%	Range	SD	Cu Pt Bi
S	17.55	17.25–18.19	0.05	17.06
Cu	12.98	12.70–13.27	0.07	11.27
Pd	2.69	2.30–3.30	0.04	–
Pt	30.04	29.12–30.69	0.02	34.06
Bi	37.65	36.96–38.05	0.02	37.07
Total	100.91	99.94–101.8		100.00

from two grains of lisiguangite. The reflectance date and color values for lisiguangite were analyzed and are given in Tables 1 and 2.

6 Chemical Data

The following X-ray lines and standards were used: S K_α (nature pyrite), Cu K_α (pure Cu), Pd L_α (pure Pd), Pt L_α (pure Pt), Bi L_α (pure Bi). 8 microprobe analyses were carried out by means of JEOL JXA-8100 (WDS mode, 20 kV, 20 nA, a beam diameter of 2 μm and counting times of 50–100 s). The average analytical results on 8 different particles in polished sections are given in Table 3. The empirical formula (based on 6 *apfu*) is $Cu_{1.10}(Pt_{0.83}Pd_{0.14})_{\Sigma 0.97}Bi_{0.97}S_{2.96}$. The ideal formula is $CuPtBiS_3$ which requires: Cu 11.27, Pt 34.60, Bi 37.07, S 17.06 (total 100.0 wt/%).

7 Crystallography

Single-crystal X-ray studies present the following data:

Orthorhombic: Space group: $P2_12_12_1$.

a=7.7152(15)Å, b=12.838(3)Å, c=4.9248(10)Å, V=487.79(17)Å^3, Z=4.

X-ray powder-diffraction data (57.3 mm diameter Debye-Scherrer camera, Cu $K\alpha_1$) are given in Table 4. The Unit-cell data refined from the powder data are as follows:

Orthorhombic, Space group: $P2_12_12_1$, a=7.685(3)Å, b=12.882(5)Å, c=4.9243(10)Å, V=487.54(11)Å^3, Z=4.

Space group $P2_12_12_1$ was obtained from the systematic absence of the following reflections: *h k l=P, 0 k l=P, h 0 l=P, h 0 l=P, h k 0=P, h 0 0=2, 0 k 0=2, 0 0 l=2.*

8 Crystal Structure

The crystal structure (Fig. 2a–c) of lisiguangite has been solved from intensity data of a single-crystal fragment (60×40×30 μm), which were collected on a Rigaku R-axis Rapid IP diffractometer with Mo $K\alpha$ radiation, at 293(2) K, in the 2θ range 6°–55°. The structure was solved in the space group $P2_12_12_1$ using SHELXS97 and SHELXL97 respectively, and refined using a full-matrix refinement on F^2 to final R indices $I>2\sigma(I)$, and R_1=0.2204 and

Table 4 X-ray power – diffraction data for lisiguangite

I	d_{meas}	$d_{cal.}$	*h k l*
30	6.40	6.44	020
20	5.93	4.937	120
10	4.60	4.600	011
5	4.20	4.146	101
5	3.94	3.947	111
5	3.74	3.749	130
10	3.49	3.486	121
80	3.24	3.236	031
100	3.03	3.029	201
20	2.87	2.863	230
20	2.73	2.741	221
5	2.55	2.543	141
10	2.46	2.462	002
40	2.27	2.283	051
50	2.14	2.140	250
25	2.05	2.058	132
20	1.920	1.921	400
60	1.865	1.867	232
5	1.780	1.780	052
10	1.750	1.754	430
10	1.639	1.641	332
10	1.591	1.593	113
10	1.505	1.510	203
		1.490	262
20	1.463	1.467	501
		1.436	143
5	1.430	1.430	371
30	1.423	1.424	233
7	1.335	1.335	541

wR_2=0.5179; *R* indices (all data) R_1=0.2338, wR_2=0.5426; observed reflection with 2010/1003 [(R_{int})=0.2918]; 55 parameters, 0 restraints; extinction coefficient, goodness of fit on *F* 1.038.

The *M*(1) sites are occupied by Cu, which is tetrahedrally coordinated by sulfur with <Cu(1)-S(1)>=2.30(3)Å (average). The *M*(2) sites are occupied by sixfold coordinated Pt^{2+}, coordinated by four S atoms in the quadratic base and two Bi atoms at the vertices of a tetragonal dipyramid with <Pt(1)-S(1) =2.36(2)Å.

The Bi atoms are coordinated by four sulfur atoms to form a trigonal pyramid. Three of the four Bi-S bond lengths are in a range closest to S atoms with <Bi(1)-S(1), (2), (3)>=2.62–2.72(2)Å; the fourth S atom is at a greater distance with <Bi (1)-S(1)>=2.92(3)Å.

The crystal structure is illustrated in Fig. 2a–c.

Atomic corrdinate and bond lengths are listed in Table 5 and Table 6.

Table 5 Atomic corrdinates ($\times10^{-4}$) and equivalent isotropic displacement parameters ($Å^2\times10^{-3}$) for q. U(eq) is defined as one third of the trace of the orthogonalized U_{ij} tensor. Anisotropic displacement paramenters ($Å^2\times10^{-3}$) for q. The anisotropic displacement factor exponent takes the form:

$-2\pi^2[h^2a^{*2}U_{11}+...+2hka^*b^*U_{12}]$

Atom	Bi(1)	Pt(1)	Cu(1)	S(1)	S(2)	S(3)
x	3817(5)	1311(4)	3904(16)	1330(30)	3810(30)	1360(30)
y	1306(3)	2499(3)	4423(10)	4121(18)	2979(18)	890(20)
Z	9150(7)	5049(7)	9700(20)	7270(50)	2520(50)	2670(50)
U(eq)	21(1)	16(1)	29(3)	26(5)	24(5)	28(5)
Atom	Bi(1)	Pt(1)	Cu(1)	S(1)	S(2)	S(3)
U11	15(2)	11(2)	23(6)	29(13)	19(10)	23(12)
U22	37(2)	28(2)	51(8)	28(9)	45(11)	44(11)
U33	9(2)	9(2)	14(5)	23(11)	8(8)	16(10)
U23	−1(1)	−1(1)	7(5)	−2(8)	6(8)	3(9)
U13	0(1)	0(1)	−1(6)	22(14)	−19(11)	0(12)
U12	−1(1)	2(1)	−12(5)	1(8)	17(9)	−1(9)

9 Relation to Other Species

Lisiguangite is a member of the lapieite group, the Pt-dominant analogue of mückeite as compared in Table 7.

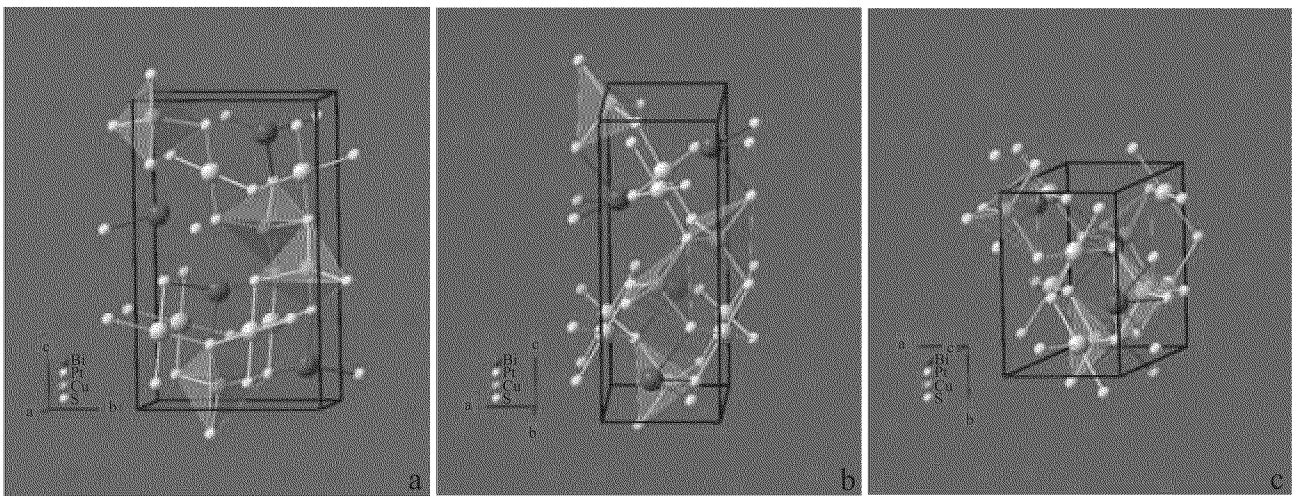

Fig. 2. Crystal structure of lisiguangite.

(a) Projected along [100]; (b) projected along [010]; (c) projected along [001].Green,Cu; white, Pt; red, Bi; yellow, S.

Table 6 Bond lengths [A] and angles [deg] for q.

Bi(1)-S(3)#1	2.62(3)	S(2)#5-Pt(1)-S(1)	90.1(8)
Bi(1)-S(1)#2	2.68(2)	S(2)#5-Pt(1)-S(3)	92.2(9)
Bi(1)-S(2)#1	2.72(2)	S(1)-Pt(1)-S(3)	177.6(9)
Bi(1)-S(3)#3	2.92(3)	S(2)#5-Pt(1)-S(2)	179.1(7)
Bi(1)-Pt(1)	3.188(4)	S(1)-Pt(1)-S(2)	90.4(8)
Bi(1)-Pt(1)#4	3.214(4)	S(3)-Pt(1)-S(2)	87.4(9)
Pt(1)-S(2)#5	2.35(2)	S(2)#5-Pt(1)-Bi(1)	92.9(7)
Pt(1)-S(1)	2.35(2)	S(1)-Pt(1)-Bi(1)	97.3(7)
Pt(1)-S(3)	2.37(3)	S(3)-Pt(1)-Bi(1)	83.4(6)
Pt(1)-S(2)	2.38(3)	S(2)-Pt(1)-Bi(1)	87.9(5)
Pt(1)-Bi(1)#5	3.214(4)	S(2)#5-Pt(1)-Bi(1)#5	87.8(7)
Cu(1)-S(1)#6	2.26(3)	S(1)-Pt(1)-Bi(1)#5	83.1(7)
Cu(1)-S(3)#4	2.27(3)	S(3)-Pt(1)-Bi(1)#5	96.2(6)
Cu(1)-S(2)#1	2.32(3)	S(2)-Pt(1)-Bi(1)#5	91.5(5)
Cu(1)-S(1)	2.35(3)	Bi(1)-Pt(1)-Bi(1)#5	179.25(13
S(1)-Cu(1)#7	2.26(3)	S(1)#6-Cu(1)-S(3)#4	120.3(11)
S(1)-Bi(1)#8	2.68(2)	S(1)#6-Cu(1)-S(2)#1	108.9(10)
S(2)-Cu(1)#9	2.32(3)	S(3)#4-Cu(1)-S(2)#1	101.0(10)
S(2)-Pt(1)#4	2.35(2)	S(1)#6-Cu(1)-S(1)	110.6(8)
S(2)-Bi(1)#9	2.72(2)	S(3)#4-Cu(1)-S(1)	114.3(10)
S(3)-Cu(1)#5	2.27(3)	S(2)#1-Cu(1)-S(1)	98.6(9)
S(3)-Bi(1)#9	2.62(3)	Cu(1)#7-S(1)-Cu(1)	102.5(10)
S(3)-Bi(1)#10	2.92(3)	Cu(1)#7-S(1)-Pt(1)	118.2(11)
		Cu(1)-S(1)-Pt(1)	112.9(11)
S(3)#1-Bi(1)-S(1)#2	92.7(8)	Cu(1)#7-S(1)-Bi(1)#8	118.5(11)
S(3)#1-Bi(1)-S(2)#1	75.7(8)	Cu(1)-S(1)-Bi(1)#8	108.0(10)
S(1)#2-Bi(1)-S(2)#1	76.1(6)	Pt(1)-S(1)-Bi(1)#8	96.8(8)
S(3)#1-Bi(1)-S(3)#3	86.3(6)	Cu(1)#9-S(2)-Pt(1)#4	119.3(12)
S(1)#2-Bi(1)-S(3)#3	90.0(7)	Cu(1)#9-S(2)-Pt(1)	123.0(9)
S(2)#1-Bi(1)-S(3)#3	156.5(7)	Pt(1)#4-S(2)-Pt(1)	109.4(9)
S(3)#1-Bi(1)-Pt(1)	94.5(5)	Cu(1)#9-S(2)-Bi(1)#9	105.4(9)
S(1)#2-Bi(1)-Pt(1)	162.7(5)	Pt(1)#4-S(2)-Bi(1)#9	96.0(7)
S(2)#1-Bi(1)-Pt(1)	90.4(4)	Pt(1)-S(2)-Bi(1)#9	96.7(9)
S(3)#3-Bi(1)-Pt(1)	106.2(5)	Cu(1)#5-S(3)-Pt(1)	113.5(11)
S(3)#1-Bi(1)-Pt(1)#4	162.6(6)	Cu(1)#5-S(3)-Bi(1)#9	107.4(10)
S(1)#2-Bi(1)-Pt(1)#4	95.0(6)	Pt(1)-S(3)-Bi(1)#9	99.4(9)
S(2)#1-Bi(1)-Pt(1)#4	91.0(6)	Cu(1)#5-S(3)-Bi(1)#10	85.1(9)
S(3)#3-Bi(1)-Pt(1)#4	109.3(5)	Pt(1)-S(3)-Bi(1)#10	135.9(10)
Pt(1)-Bi(1)-Pt(1)#4	74.12(7)	Bi(1)#9-S(3)-Bi(1)#10	113.2(9)

Symmetry transformations used to generate equivalent atoms:
#1 x, y, z+1; #2 x+1/2, −y+1/2, −z+2; #3 −x+1/2, −y, z+1/2; #4 x+1/2, −y+1/2, −z+1; #5 x−1/2, −y+1/2,−z+1; #6 −x+1/2,−y+1, z+1/2; #7 −x+1/2,−y+1, z−1/2; #8 x−1/2,−y+1/2,−z+2; #9 x, y, z−1, #10 −x+1/2,−y, z−1/2.

Table 7 Comparative data for lapieite-group minerals

Mineral	Lisiguangite	Mückeite	Lapieite
Formula	$CuPtBiS_3$	$CuNiBiS_3$	$CuNiSbS_3$
Symmetry	$P2_12_12_1$	$P2_12_12_1$	$P2_12_12_1$
*a*Å	7.685(3)	7.514(3)	7.422(2)
*b*Å	12.882(5)	12.557(6)	12.508(3)
*c*Å	4.9243(3)	4.880(2)	4.900(1)
*V*Å^3	487.5(5)	459.7(2)	454.9
Z	4	4	4
Strong lines of XPD *dÅ(I, %, hkl)*	3.24(80)031 3.03(100)201 2.14(50)250 1.865(60)232	3.177(80)031 2.975(100)201 2.087(60)250 1.837(70)232	3.178(90)031 2.959(100)201 2.073(20)250 1.837(90)232
D (calc.) g/cm^3	7.42	5.88	4.966
Reference	This work	Schnorrer-köhler et al., 1989	Harris et al., 1987

Acknowledgements

Thanks are due to Dr Lin Shengzhong and Qu Guolin, and Professors of the Institute of Mineral Resources, CAGS for carrying out X-ray powder-diffraction with the Debye-Scherrer camera for lisiguangite. We also appreciate Dr Shu Guiming, Professor of Beijing University, for assistance with the electron microprobe analysis for lisiguangite.

Manuscript received Jan. 12, 2009
accepted Jan. 22, 2009
edited by Liu Xinzhu

References

Harris, D.C., Roberts, A.C., Thorpe, R.R., Jonasson, I.R., and Criddle, A.J., 1984. Lapieite, $CuNiSbS_3$, a new mineral species from the Yukon territory. *Can. Min.*, 22: 561–564.

Schnorrer-köhler, G., Neumann, U., and Doering, Th., 1989. Mückeite, $CuNiBiS_3$, a new ore mineral from the Grüne Au mine, Schutzbach /Siegerland. Stuttgart: *Neues Jahrb. Mineral, Monatsh.* 5: 193–200.

Yu Zuxiang and Ding Kuishou and Zhou Jianxiaong, 1978. Daomanite, a new platinum mineral. *Acta Geologica Sinica* (English edition), 52(4): 320–325.

Yu Zuxiang, 1997. Yixunite, an ordered new native Indium and Platinum Alloy. *Acta Geologica Sinica* (English edition), 71 (4): 328–331.

Yu Zuxiang, Wei Jiuaxiu and Liu Yan, 2002. A new kind of PEG deposit—the Village of Sandao type of contact metasomatism deposit and its ore mineralogy. *Papers from the 18th General Meeting, Edinburgh, Scotland*, 286–287.

Explanation of the Plate

Plate I Morphology of crystal of lisiguangite
(scanning electron microscopy [SEM] images)
(a) Idiomorphic tabular lisiguanite (lsg, green);
(b) Idiomorphic tabular lisiguanite (lsg, brownish red);
(c) Tabular lisiguangite (lsg, yellow);
(d) Massive fragment of lisiguangite (lsg, green)
(note the perfect {010}, {100} cleavage);
(e) Idiomorphic tabular fragment of lisiguanite (lsg, brownish red);
(f) Imbricated structure lisiguanite (lsg, red).

Plate II Scanning electron microscopy (SEM) images of lisiguangite associated with other minerals.
(a) Tabular lisiguangite (lsg, yellow) intergrown with daomanite (dam, yellowish green);
(b) on its tabular cleavage, lisiguangite (lsg, orange) is replaced by idiomorphic Co-bearing malanite (Co-mal, reddish orange);
(c) massive lisiguangite (lsg, red) is replaced by daomanite (dam, green), and Co-bearing malanite (Co-mal, blue);
(d) massive Co-bearing malanite (Co-mal, blue) is replaced by lisiguangite (lsg, bluish white);
(e) lisiguangite (lsg, red) may be intergrown with malyshevite (mlv, dark red);
(f) idiomorphic lisiguangite (lsg, white) is replaced by tenoite (tnr, blue).

Plate I Morphology of crystal of lisiguangite (scanning electron microscopy [SEM] images)

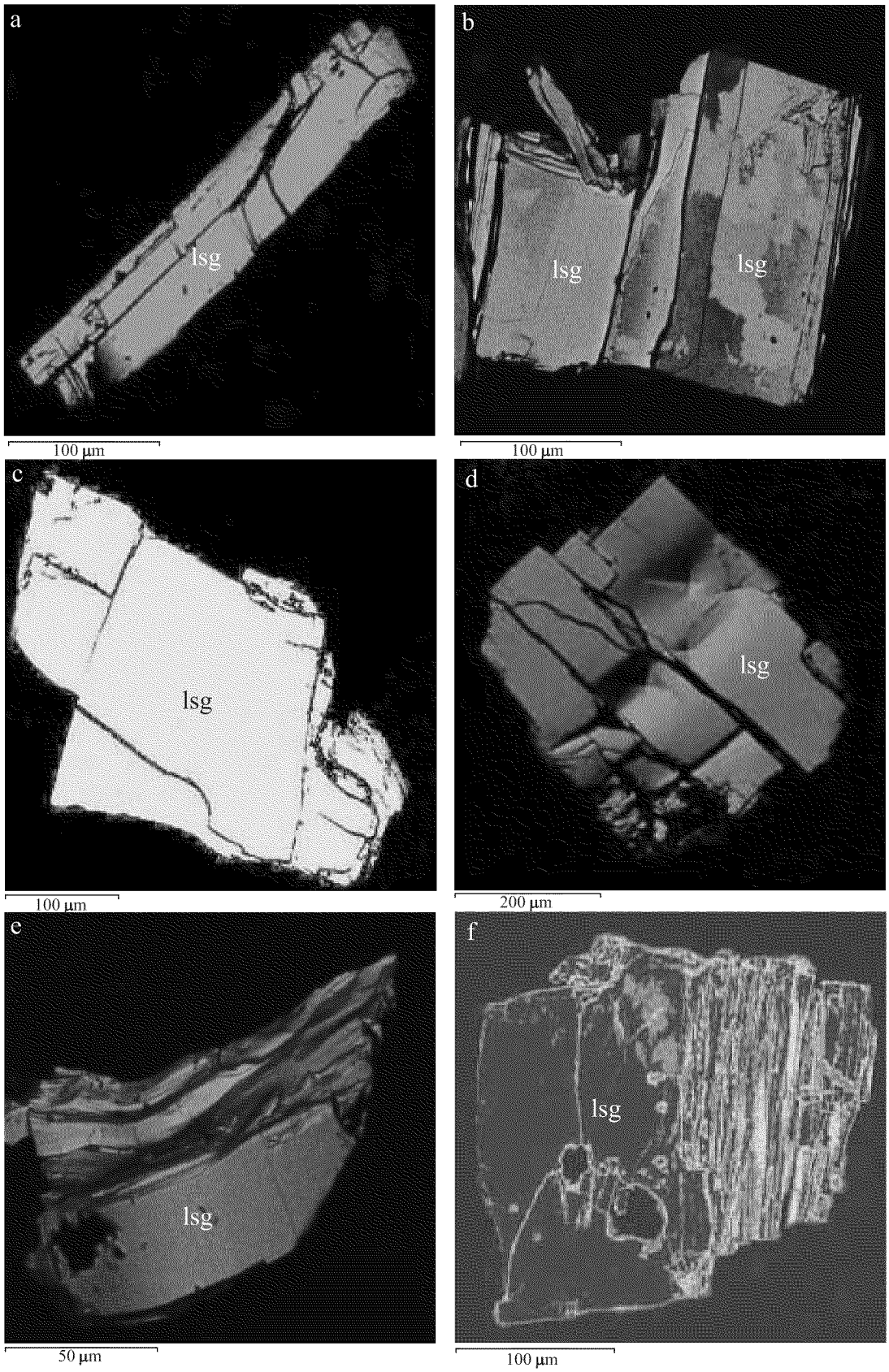

Plate II Scanning electron microscopy (SEM) images of lisiguangite associated with other minerals